

As shown in Table 1, the rate of production of ethylbenzene was maximum for the catalyst with the largest Mo–Mo and Mo–S coordination numbers. This is in agreement with results obtained earlier in this laboratory (3) that showed a similar relationship between the rate of HDS of thiophene and Mo–S coordination number determined in a less precise way.

We have observed a double correlation under real conditions of operation and with a working catalyst between HDS activity on the one hand and catalyst composition and structure on the other hand. Further work is under way to determine the nature of this correlation.

M. BOUDART  
R. A. DALLA BETTA  
K. FOGER  
D. G. LÖFFLER  
M. G. SAMANT

Department of Chemical Engineering,  
Stanford University, Stanford,  
California 94305

#### References and Notes

1. B. G. Silbernagel, T. A. Pecoraro, R. R. Chianelli, *J. Catal.* **78**, 380 (1982).
2. F. E. Massoth *et al.*, *ibid.* **85**, 53 (1984).
3. M. Boudart, J. Sánchez Arrieta, R. A. Dalla Betta, *J. Am. Chem. Soc.* **105**, 295 (1984).
4. B. S. Clausen, H. Topsøe, R. Candia, B. Lengeler, *ACS Symp. Ser.* **24**, 71 (1984).
5. T. G. Perham and R. P. Merrill, *J. Catal.* **85**, 295 (1984).
6. J. H. Sinfelt, *Bimetallic Catalysts: Discoveries, Concepts, and Applications* (Wiley, New York, 1983), pp. 63–82 and 98–111.
7. K. Tamaru, *Dynamic Heterogeneous Catalysis* (Academic Press, London, 1978), pp. vii and viii.
8. M. Boudart, R. Dalla Betta, K. Foger, D. G. Löffler, *Springer Proc. Phys.* **2**, 187 (1984).
9. B. C. Gates, J. R. Katzer, G. C. A. Schuit, *Chemistry of Catalytic Processes* (McGraw-Hill, New York, 1979), pp. 390–422.
10. R. A. Dalla Betta, M. Boudart, K. Foger, D. G. Löffler, J. Sánchez Arrieta, *Rev. Sci. Instr.* **55**, 1910 (1984).
11. P. A. Lee, P. H. Citrin, P. Eisenberger, B. M. Kincaid, *Rev. Mod. Phys. Part 1* **53**, 769 (1981).
12. Supported by grant DE-FG22-83PC60782 from the U.S. Department of Energy (Fossil Energy Division) and carried out in part at the Stanford Synchrotron Radiation Laboratory (supported by the U.S. Department of Energy). K.F., on leave from the Commonwealth Scientific and Industrial Research Organization, Division of Materials Science (Australia), and D.G.L., on leave from the Universidad Nacional de Mar del Plata and Consejo Nacional de Investigaciones Científicas y Técnicas (Argentina), acknowledge support from their home organizations.

17 December 1984; accepted 13 February 1985

## Coupling of *Tetrahymena* Ribosomal RNA Splicing to $\beta$ -Galactosidase Expression in *Escherichia coli*

**Abstract.** *Splicing of the Tetrahymena ribosomal RNA precursor is mediated by the folded structure of the RNA molecule and therefore occurs in the absence of any protein in vitro. The Tetrahymena intervening sequence (IVS) has been inserted into the gene for the  $\alpha$ -donor fragment of  $\beta$ -galactosidase in a recombinant plasmid. Production of functional  $\beta$ -galactosidase is dependent on RNA splicing in vivo in Escherichia coli. Thus RNA self-splicing can occur at a rate sufficient to support gene expression in a prokaryote, despite the likely presence of ribosomes on the nascent RNA. The  $\beta$ -galactosidase messenger RNA splicing system provides a useful method for screening for splicing-defective mutations, several of which have been characterized.*

Many eukaryotic genes contain introns, or intervening sequences (IVS), that must be removed from their RNA transcripts by a cleavage-ligation reaction termed RNA splicing (1). In one class of splicing reactions the RNA mediates its own splicing. Examples include the nuclear ribosomal RNA (rRNA) precursor of the ciliated protozoan *Tetrahymena* (2, 3), as well as various mitochondrial messenger RNA (mRNA) and rRNA precursors in fungi (4). The RNA lowers the activation energy for specific cleavage-ligation reactions by providing a binding site for guanosine, one of the reactants, and by straining or activating the phosphates at the splice sites (5, 6). In addition, a portion of the IVS may bind one or both adjacent rRNA coding regions (exons) to facilitate their ligation (7).

RNA self-splicing in vitro requires

only monovalent and divalent cations and some form of the nucleoside guanosine (2, 3). We therefore reasoned that it should take place to some extent in vivo, even in a prokaryotic cell where RNA splicing is not a normal feature of gene expression. We have now tested this idea by inserting the *Tetrahymena* IVS and a small portion of the exons within sequences coding for  $\beta$ -galactosidase. Both genetic and physical evidence support the conclusion that accurate RNA splicing occurs in *E. coli* to produce functional mRNA. The system has been used to isolate mutants that are defective in splicing. Thus, classical genetic techniques can now be used to investigate structure-function relations in the self-splicing IVS.

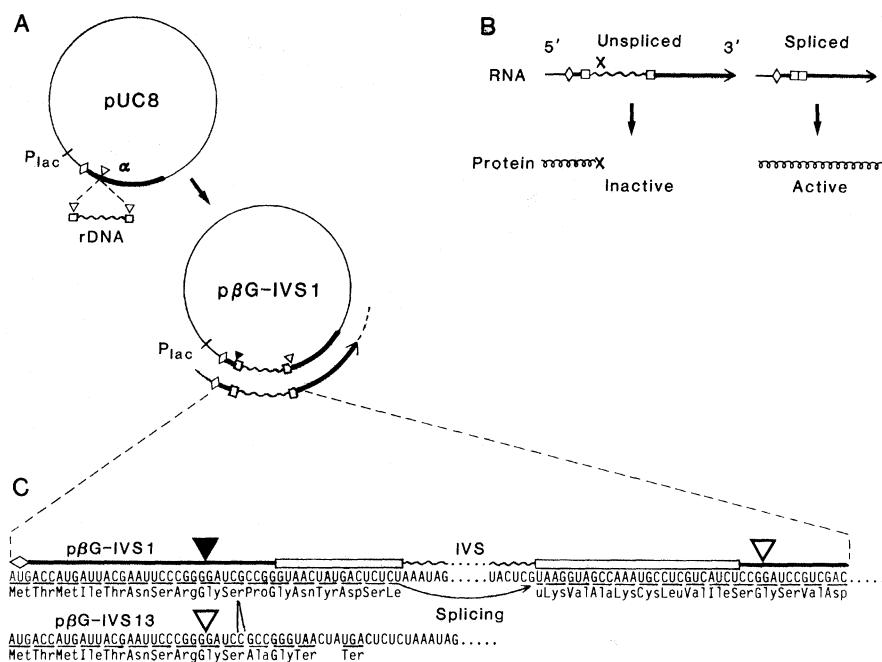
Plasmid pUC8 encodes the NH<sub>2</sub>-terminal portion ( $\alpha$ -donor fragment) of the  $\beta$ -galactosidase protein (8). The  $\alpha$ -donor

polypeptide can combine with a defective  $\beta$ -galactosidase protein ( $\alpha$ -acceptor) to restore enzyme activity (9). A fragment of the *Tetrahymena* rRNA gene containing the IVS was inserted in the Bam HI restriction site within the  $\alpha$ -donor coding region of pUC8 (Fig. 1A). The 413-nucleotide IVS contains stop codons in all three reading frames, which would cause premature termination of  $\alpha$ -donor translation. If RNA splicing occurred, however, the small portions of the exons included in the insert would be joined to give an open reading frame. Extra amino acids can be tolerated in the  $\alpha$ -donor fragment without destroying activity. Thus,  $\beta$ -galactosidase expression would be contingent on RNA splicing (Fig. 1B).

*Escherichia coli* strain JM83 (8) was transformed with the recombinant plasmids and plated on agar containing ampicillin and X-gal (5-bromo-4-chloro-3-indolyl- $\beta$ -D-galactoside). X-gal is a histochemical substrate for  $\beta$ -galactosidase and is converted to a blue dye after hydrolysis by the enzyme. Approximately half of the colonies were white (no  $\beta$ -galactosidase expression); the remainder were mostly very pale blue, while a few were blue. Restriction endonuclease cleavage analysis of plasmids from three colonies of each color group indicated that the white colonies contained the *Tetrahymena* insert in the incorrect orientation, whereas the blue and very pale blue colonies contained the insert in the correct orientation. Nucleotide sequencing of plasmids from three blue colonies (including p $\beta$ G-IVS1) indicated that in each case one nucleotide had been inserted at the upstream Bam HI site during cloning (Fig. 1C). The deletion was such that the open reading frame of the ligated exons was put in-frame with the  $\beta$ -galactosidase coding sequences. Translation of the resulting mRNA would give an  $\alpha$ -donor polypeptide containing 18 amino acids more than that produced by pUC8, and should give  $\beta$ -galactosidase activity (10). In the plasmids from the very pale blue colonies, such as p $\beta$ G-IVS13, both Bam HI sites were intact (Fig. 1C). Sequencing indicated two termination codons in the protein reading frame, which should eliminate  $\beta$ -galactosidase activity (8). The residual  $\beta$ -galactosidase activity conferred by these plasmids may be due to occasional splicing to a site upstream from the termination codons in the correct reading frame.

Several lines of evidence indicate that production of  $\beta$ -galactosidase in p $\beta$ G-IVS1 is dependent on proper splicing of the  $\alpha$ -donor pre-mRNA. The extra nu-

Fig. 1. Plasmid constructed to obtain splicing-dependent expression of  $\beta$ -galactosidase. (A) A Bam HI restriction fragment containing the *Tetrahymena* ribosomal RNA gene IVS and small portions of the adjoining exons was inserted into the Bam HI restriction site in the multiple cloning site of pUC8 (8) such that the  $\alpha$ -donor coding sequences were interrupted. The *Tetrahymena* fragment was isolated from pJE457, which had been constructed from pIVS11 (3) by deletion of most of the exons and the addition of synthetic Bam linkers. (Thick line)  $\alpha$ -Donor coding sequences; (wavy line) IVS; (diamond) initiation codon for  $\alpha$ -donor protein synthesis; (squares) *Tetrahymena* exon sequences; (open triangles) Bam HI restriction sites; (filled triangle) position of the Bam HI restriction site that was destroyed during cloning of p $\beta$ G-IVS1. (B) Model describing the expected translation products of p $\beta$ G-IVS1 transcripts with and without RNA splicing. (X) Stop codon in the RNA that causes premature termination of the  $\alpha$ -donor polypeptide. The first such codon is at nucleotides 62 to 64 past the 5' splice site. (C) DNA sequences determined by the dideoxynucleotide method (18). The 5' region was sequenced by extension of a primer complementary to nucleotides 67–83 of the IVS and confirmed by sequencing the opposite strand with the M13 reverse sequencing primer (19). The 3' region was sequenced with the M13 sequencing primer (Bethesda Research Laboratories, 1211). Only one open reading frame (codons underlined) extends through the *Tetrahymena* exon sequences.



cleotide present in p $\beta$ G-IVS13 relative to p $\beta$ G-IVS1 results in the elimination of most of the  $\beta$ -galactosidase activity, consistent with most of the translation starting at the normal AUG (A, adenine; U, uracil; G, guanine) initiation codon. If the functional  $\alpha$ -donor fragment were made from some AUG brought in with the *Tetrahymena* insert, the two plasmids should produce equal amounts. Non-overlapping deletions within the IVS that eliminate splicing activity also eliminate  $\beta$ -galactosidase expression (see below), and thus provide additional evidence that splicing is required for expression. The effect of these deletions cannot be explained by the elimination of some hypothetical site for reinitiation of protein synthesis within the IVS, because the remaining portion of the IVS downstream from the deletions contains stop codons in all reading frames.

The efficacy of the system for isolation of splicing-defective mutants was tested. Plasmid p $\beta$ G-IVS1 DNA was linearized at either of two single-copy restriction endonuclease cleavage sites within the IVS, the Sph I site at position 42 of the IVS or the Bgl II site at position 236. Deletions were made with nuclease BAL 31. When cells were transformed and assayed on X-gal plates, colonies ranging in color from blue to pale blue and white were obtained. The frequency of colonies expressing  $\beta$ -galactosidase decreased as the average extent of deletion increased. Deletion of an average of 13 nucleotides from the Sph I site or of 25

nucleotides from the Bgl II site eliminated activity in 75 percent of the colonies.

Plasmids were isolated and subjected to nucleotide sequence analysis (Table 1). There was a good correlation be-

Table 1. Small deletions within the IVS eliminate  $\beta$ -galactosidase activity. Plasmids containing deletions were constructed as described (11). The p $\beta$ GB and p $\beta$ GS plasmids have deletions from the Bgl II and Sph I sites of p $\beta$ G-IVS1, respectively. Colonies showing a range of  $\beta$ -galactosidase activity were picked and grown in liquid culture. Plasmid DNA was isolated (20) and sequenced by the dideoxynucleotide method (18). A primer complementary to nucleotides 274 to 288 of the IVS was used to sequence the deletions from the Bgl II site, and a primer complementary to nucleotides 67 to 83 was used to sequence the deletions from the Sph I site. Nucleotide, nt.

Plasmid	Color	Deletion	
		Position	Size (nt)
p $\beta$ GB-3	Blue	230–245	16
p $\beta$ GB-14	Pale blue	230–240	11
p $\beta$ GB-2	Pale blue	226–240	15
p $\beta$ GB-49*	Pale blue	225–241	17
p $\beta$ GB-43	Paler blue	225–247	23
p $\beta$ GB-4	White	226–251	26
p $\beta$ GB-5*	White	225–251	27
p $\beta$ GB-7	White	219–252	34
p $\beta$ GS-2	Blue	–	0
p $\beta$ GS-1†	Pale blue	41–44	4
p $\beta$ GS-8*	White	41–49	9
p $\beta$ GS-7	White	41–55	15
p $\beta$ GS-17	White	20–62	43

\*Two independent isolates of each of these deletions. †Five independent isolates of this deletion.

tween  $\beta$ -galactosidase activity in vivo and self-splicing activity in vitro. The deletion of nucleotides 230 through 245 in p $\beta$ GB-3 largely removes stem-loop element "f" in the IVS secondary structure (12) but retains full  $\beta$ -galactosidase activity, consistent with our previous conclusion that stem-loop "f" is dispensable for self-splicing (11). The deletion of nucleotides 230 through 240, a smaller deletion that removes only part of stem-loop "f", has reduced  $\beta$ -galactosidase activity. The remaining nucleotides may lead to the formation of a counterproductive structure. This, however, was an exception; in general, increasing deletion size correlated with loss of enzyme activity. Plasmid p $\beta$ GB-43 ( $\Delta$ 225–247) gives a pale blue colony, and a very similar construct (pGK $\Delta$ 225–248) has about 2 percent of normal splicing activity in vitro (11). The plasmids p $\beta$ GB-4 ( $\Delta$ 226–251) and p $\beta$ GB-5 ( $\Delta$ 225–251) give white colonies, while a construct with a slightly larger deletion (pGK $\Delta$ 224–252) has been shown to have very low activity (<2 percent) in vitro (11). Thus, for these mutants the limit of detection of  $\beta$ -galactosidase activity corresponds to about 2 percent residual self-splicing activity.

Deletions from the Sph I site affect stem-loop element "b" (nucleotides 31 to 40 pairing with 47 to 56) in the IVS secondary structure (12). We previously found that constructs missing nucleotides 41 to 44 in the hairpin loop had approximately normal splicing activity, whereas larger deletions that destabi-

lized the stem had substantially reduced activity (11). The same trend is seen with  $\beta$ -galactosidase activity in Table 1: p $\beta$ GS-1 has somewhat reduced activity, while p $\beta$ GS-8 and p $\beta$ GS-7 have no detectable activity.

Clearly the amount of  $\beta$ -galactosidase activity could depend on factors other than intrinsic self-splicing activity of the RNA. Thus, structural alterations of the IVS that lead to very rapid degradation of precursor RNA by cellular nucleases could produce a  $\beta$ -galactosidase-deficient phenotype without being altered in splicing efficiency. Mutants obtained in vivo must therefore be assayed for splicing in vitro before firm conclusions can be drawn.

Analysis of the steady-state RNA population in cells harboring the various plasmids provided additional evidence for RNA splicing in *E. coli*, and evidence that splicing follows the same pathway described for *Tetrahymena* (2, 13, 14). Cells containing p $\beta$ G-IVS1 had a large amount of RNA that hybridized to an IVS probe (Fig. 2). A small portion of this RNA was authentic excised linear IVS RNA, as judged by the following criteria. It was the correct size (resolved within five nucleotides); it underwent autocyclization (Fig. 2A), evidence of a correct 3' end and a free 3' hydroxyl group (14); and it had the same 5' end as the intact linear IVS, including the extra nucleotide added during IVS excision (Fig. 2B and additional data not shown). A small amount of IVS RNA was also observed to migrate as the circular species.

The major portion of the IVS-specific RNA appeared on the ethidium-stained polyacrylamide gel as a closely spaced doublet of bands, indicated by the arrow in Fig. 2A. One band was measured to be about 20 nucleotides smaller than authentic excised IVS RNA and one about 25 nucleotides smaller. Nucleotide sequence analysis showed that this RNA had two distributions of 5' ends at nucleotides 18 to 21 and 23 to 26 (Fig. 2B). These results were confirmed by sequence analysis of the isolated RNA. Thus, these molecules are not the L-15 and L-19 IVS RNA products of self-catalyzed hydrolysis of circular IVS characterized previously (6). It is likely that the heterogeneous 5' ends are produced by the action of cellular nucleases on linear IVS RNA. Alternatively, it is possible that this RNA never underwent splicing, and is simply the nuclease-resistant core resulting from degradation of the precursor RNA in *E. coli*. Finally, there was a diffuse band of IVS-containing RNA of higher molecular weight.

This RNA also hybridized to a probe to the 3' exon (data not shown), and is presumably the  $\alpha$ -donor pre-mRNA.

Blot hybridization with RNA from cells containing p $\beta$ G-IVS13 showed an amount of IVS RNA comparable to that found in cells containing p $\beta$ G-IVS1 (Fig. 2C), consistent with the loss of  $\beta$ -galactosidase activity being due to early termination of translation and not to some defect in splicing or transcription. Blot hybridization was also performed on RNA from cells containing plasmids with deletions in the IVS (Fig. 2C). The size of the IVS RNA decreased in proportion to the size of the deletion, as expected. The abundance of the IVS RNA in the cells did not necessarily correlate with the amount of  $\beta$ -galactosidase activity,

perhaps because of differential RNA stability in vivo. RNA from one white colony (p $\beta$ GB-4) contained a small amount of large IVS-containing RNA but no detectable excised IVS RNA.

In conclusion, it appears that accurate splicing of the *Tetrahymena* IVS occurs in *E. coli*. Splicing in *E. coli* appears to follow the pathway described in vitro, including the highly characteristic addition of a nucleotide to the 5' end of the excised IVS RNA. Although *Tetrahymena* pre-rRNA splicing has minimal requirements in vitro, it is somewhat surprising that it takes place in *E. coli* with high enough efficiency to support  $\beta$ -galactosidase expression. Unlike eukaryotes, bacteria have coupled transcription-translation; the presence of ribo-

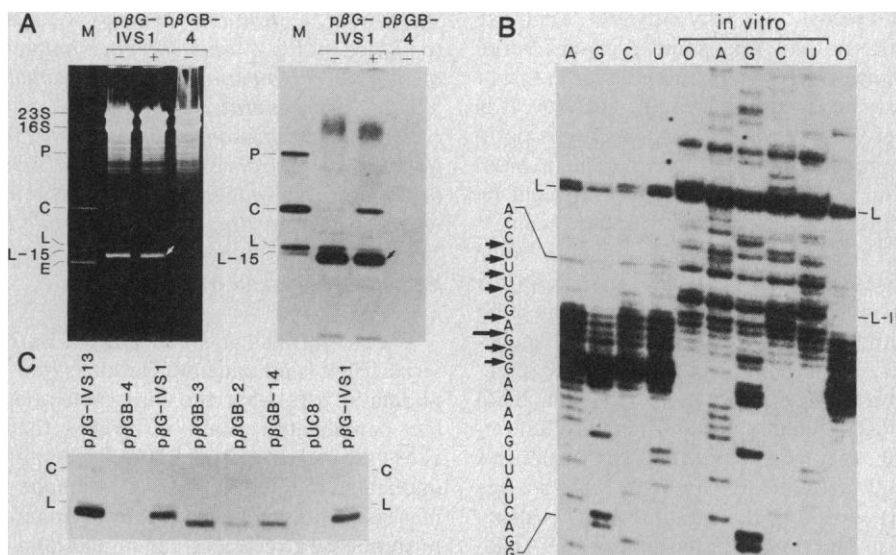


Fig. 2. Identification of IVS-containing RNA species in *E. coli* by RNA blot hybridization and primer extension. (A) RNA was purified from *E. coli* containing various plasmids. RNA (20- $\mu$ g samples) was fractionated by electrophoresis in a 4 percent polyacrylamide, 8M urea gel and visualized by ethidium bromide staining. The gel was soaked in 100 mM NaOH for 20 minutes, and neutralized in phosphate buffer, pH 6.5; the RNA was electrophoretically transferred to Gene Screen (New England Nuclear). Hybridization was performed with a  $^{32}$ P-labeled oligodeoxynucleotide complementary to nucleotides 67 to 83 of the IVS. (Left) Ethidium bromide-stained gel. (Right) Autoradiogram showing IVS-containing RNA. (+) Purified RNA incubated in 200 mM sodium acetate, 10 mM MgCl<sub>2</sub>, 30 mM tris, pH 7.5, 0.1 percent sodium dodecyl sulfate, 0.30 mM GTP (guanosine triphosphate) for 30 minutes at 42°C (IVS splicing and cyclization conditions). (-) No incubation. (M) Marker RNA was transcribed in vitro from pSPTT1A3 with SP6 RNA polymerase; the resulting pre-rRNA (P, 766 nucleotides) was gel-purified and incubated for 10 minutes under splicing and cyclization conditions, giving C (circular IVS), L (linear IVS, 414 nucleotides), L-15 (reopened circle, 399 nucleotides), and E (ligated exons, 353 nucleotides). The arrow indicates the prominent doublet of IVS-containing RNA. (B) Total cellular RNA from bacteria carrying p $\beta$ G-IVS1 was analyzed by primer extension and dideoxynucleotide sequencing (18) to determine the 5' ends of IVS RNA molecules. A primer complementary to nucleotides 67 to 83 of the IVS was hybridized to RNA and extended by reverse transcriptase in the presence of all four deoxynucleoside triphosphates (11). A single ddNTP (dideoxynucleoside triphosphate) was included in each reaction. A, G, C, and U indicate the ribonucleotide complementary to the ddNTP that was added. (O) No ddNTP added. (in vitro) The same reactions were performed on products of in vitro splicing of pre-rRNA (incubated in 5 mM MgCl<sub>2</sub>, 200 mM ammonium acetate, 30 mM tris, pH 7.5, 0.20 mM GTP at 30°C for 45 minutes, conditions that favor accumulation of linear IVS RNA). Arrows at the left indicate major stops in the in vivo RNA preparation; they are interpreted to be ends of molecules. L and L-15 indicate stops corresponding to the 5' ends of the linear IVS and the L-15 IVS, which is the product of reopening of circular IVS. Molecules extending beyond the 5' splice site had the sequence of precursor RNA (not shown). Sequences were analyzed on an 8 percent polyacrylamide, 8M urea gel. (C) RNA blot hybridization as in (A), showing patterns of IVS RNA's from cells carrying various plasmids. Ethidium bromide staining of the gel (not shown) indicated equivalent amounts of cellular RNA in all lanes.

somes on the nascent pre-mRNA might be expected to interfere with proper folding of the RNA and therefore with splicing *in vivo*. Furthermore, the intrinsic rate of self-splicing is not high. It occurs with a half-life of about 1 minute at saturating concentrations of guanosine *in vitro* (5), a time that might be substantial relative to the mRNA half-life. It should be noted that the rate and the absolute efficiency of splicing *in vivo* are unknown. Because the  $\alpha$ -donor gene is present on a multiple-copy plasmid, even inefficient splicing might give full complementation of  $\beta$ -galactosidase activity.

Thus RNA splicing, generally considered to be a eukaryotic phenomenon, can take place in a prokaryote. In addition to the artificial example reported here, there may be naturally occurring cases; there is now evidence for splicing of phage T4 thymidylate synthase mRNA (15), and some archaeobacterial transfer RNA's contain insertions that may be intervening sequences (16). It is not yet clear why RNA splicing is not a more common feature of gene expression in *E. coli*, and whether it might be more common in other prokaryotes.

On a practical level, a simple color assay can now be used as a screen for splicing-deficient mutants generated by either random or site-specific mutagenesis. The system also should allow selection for second-site revertants, which are most valuable for identifying or confirming secondary and tertiary structures that facilitate splicing (17). Such studies are essential for establishing the structure-function relationships of self-splicing RNA.

JAMES V. PRICE  
THOMAS R. CECH

Department of Molecular, Cellular and Developmental Biology and Department of Chemistry, University of Colorado, Boulder 80309

#### References and Notes

1. P. Sharp, *Cell* **23**, 643 (1981); T. R. Cech, *ibid.* **34**, 713 (1983); C. L. Greer and J. Abelson, *Trends Biochem. Sci.* **9** (No. 4), 139 (1984).
2. T. R. Cech, A. J. Zaug, P. J. Grabowski, *Cell* **27**, 487 (1981); A. J. Zaug and T. R. Cech, *Nucleic Acids Res.* **10**, 2823 (1982).
3. K. Kruger *et al.*, *Cell* **31**, 147 (1982).
4. G. Garriga and A. M. Lambowitz, *ibid.* **39**, 631 (1984); G. Van der Horst and H. F. Tabak, *ibid.*, in press.
5. B. L. Bass and T. R. Cech, *Nature (London)* **308**, 820 (1984).
6. A. J. Zaug, J. R. Kent, T. R. Cech, *Science* **224**, 574 (1984).
7. R. W. Davies, R. B. Waring, J. A. Ray, T. A. Brown, C. Scazzocchio, *Nature (London)* **300**, 719 (1982); F. Sullivan *et al.*, in preparation.
8. J. Vieira and J. Messing, *Gene* **19**, 259 (1982).
9. I. Zabin and A. V. Fowler, in *The Operon*, J. H. Miller and W. S. Reznikoff, Eds. (Cold Spring Harbor Laboratory, Cold Spring Harbor, N.Y., 1978), pp. 89-121.
10. The blue color of p $\beta$ G-IVS1 was less intense than that of pUC8, but as intense as that of pUC18. Both p $\beta$ G-IVS1 and pUC18 have extra codons in the multiple cloning site relative to

- pUC8. The difference in  $\beta$ -galactosidase activity between these plasmids may be due to the extra amino acids in the proteins rather than different amounts of enzyme (8).
11. J. V. Price, G. L. Kieft, J. R. Kent, E. L. Sievers, T. R. Cech, *Nucleic Acids Res.* **13**, 1871 (1985).
  12. T. R. Cech, N. K. Tanner, I. Tinoco, B. R. Weir, M. Zuker, P. S. Perlman, *Proc. Natl. Acad. Sci. U.S.A.* **80**, 3903 (1983); F. Michel and B. Dujon, *EMBO J.* **2**, 33 (1983); T. Inoue and T. R. Cech, *Proc. Natl. Acad. Sci. U.S.A.* **82**, 648 (1985).
  13. S. L. Brehm and T. R. Cech, *Biochemistry* **22**, 2390 (1983).
  14. A. J. Zaug, P. J. Grabowski, T. R. Cech, *Nature (London)* **301**, 578 (1983).
  15. F. K. Chu, G. F. Maley, F. Maley, M. Belfort *Proc. Natl. Acad. Sci. U.S.A.* **81**, 3049 (1984); M. Belfort, personal communication.
  16. B. P. Kaine, R. Gupta, C. R. Woese, *Proc.*

17. B. Weiss-Brummer, J. Holl, R. J. Schweyen, G. Rödel, F. Kaudewitz, *Cell* **33**, 195 (1983).
18. F. Sanger, S. Nicklen, A. R. Coulson, *Proc. Natl. Acad. Sci. U.S.A.* **74**, 5463 (1977); for specific details of method see (11).
19. G. F. Hong, *Biosci. Rep.* **1**, 243 (1981).
20. D. S. Holmes and M. Quigley, *Anal. Biochem.* **114**, 193 (1981).
21. We thank Jan Engberg for his support and for providing pJE457, Art Zung for pSPTT1A3, Jan Logan for figure preparation, Udo Johanningmeier and George Weinstock for helpful discussions, and Gregg Morin for his comments on the manuscript. Supported by NIH grant GM28039, by the NIH Biomedical Research Support Grant Program, Division of Research Resources, and by an NIH Research Career Development Award (T.C.).

4 February 1985; accepted 14 March 1985

## Individual Tumors of Multifocal EB Virus-Induced Malignant Lymphomas in Tamarins Arise from Different B-Cell Clones

**Abstract.** Cotton-top tamarins were inoculated with sufficient Epstein-Barr virus to induce multiple tumors in each animal within 14 to 21 days. The tumors consisted of large-cell lymphomas that contained multiple copies of the Epstein-Barr virus genome and generated Epstein-Barr virus-carrying cell lines showing no detectable consistent chromosomal abnormality. Hybridization of tumor DNA with immunoglobulin gene probes revealed that each lymphoma was oligo- or monoclonal in origin and that individual tumors from the same animal arose from different B-cell clones. Thus the virus induced multiple transformation events in tamarins *in vivo* to cause malignant tumors resembling the Epstein-Barr virus-associated lymphomas of patients with organ transplants.

The strong links between Epstein-Barr virus (EBV) and endemic Burkitt's lymphoma suggest that the virus activates the complicated chain of events that cause the tumor (1, 2). EBV was recently implicated in the etiology of the lymphomas seen with undue frequency in immunosuppressed recipients of human allografts (3, 4). These lymphomas in transplant patients have been controversial, since most were thought to be polyclonal and therefore hyperplastic, and some have regressed (5). However, Southern blot hybridization to detect clonal immunoglobulin (Ig) gene rearrangements (6) in lymphomas from cardiac transplant recipients has shown monoclonality at first presentation (7), and thus that the tumors are best regarded as truly malignant.

The demonstration that inoculation of EBV caused lymphomas in owl monkeys and cotton-top tamarins was evidence supporting EBV oncogenicity (8). But, on the basis of conventional tests, the disease in tamarins was recently dismissed as a polyclonal lymphoproliferation (9), which is not a malignant process.

In research to develop a subunit vaccine against EBV (10), it was necessary to elaborate a virus challenge that would induce multiple lymphoid tumors in 100 percent of unprotected cotton-top tamarins.

Because of this and the disputed clonality of the resultant tumors, we have reinvestigated the tamarin lesions with reference to EBV carcinogenicity and similarities to the tumors of organ graft patients.

Cotton-top tamarins (*Saguinus oedipus oedipus*) were bred successfully in captivity (11). Suspensions of EBV were prepared from B95-8 cells (12); culture supernatants were concentrated by 2 hours of centrifugation at 100,000g and the pellet was carefully resuspended in 1 percent of the original fluid volume by drawing in and out through four graded needles of 26 to 19 gauge. The suspension was passed through a Millipore filter (pore size, 1.2  $\mu$ m) and titrated in fetal cord blood lymphocytes (13); the titrations included a virus preparation of known titer and were repeated three times to take account of variations in the sensitivity of cells from different cord blood samples. Virus suspensions with more than 10<sup>5</sup> lymphocyte-transforming doses per milliliter were selected since smaller doses did not regularly cause tumors.

We gave all the animals 10<sup>5-3</sup> lymphocyte-transforming doses. In experiment 1 inoculations were given in 4 ml of culture fluid, divided equally among intravenous, intraperitoneal, and intramuscular routes; in experiments 2 and 3